B-9-5

Extended Abstracts of the 2010 International Conference on Solid State Devices and Materials, Tokyo, 2010, pp1006-1007

Uniaxial and Biaxial Strain Distribution Mapping in SOI Micro-Structures by Polarized Raman Spectroscopy

Masashi Kurosawa[1,2], Taizoh Sadoh[1] and Masanobu Miyao[1]
[1] Department of Electronics, Kyushu University, 744 Motooka, Fukuoka 819-0395, Japan
[2] JSPS Research Fellow, 8 Ichiban-cho, Chiyada-ku, Tokyo 102-8472, Japan

Tel: +81-92-802-3737, Fax: +81-92-802-3724, E-mail: m_kurosawa@nano.ed.kyushu-u.ac.jp

1. Introduction

The micro-probe Raman scattering spectroscopy is a powerful technique to evaluate the local strain distribution induced in semiconductor. Mapping of strain fields and strain types (compressive or tensile) can be achieved without any special sample preparation. To develop the advanced MOSFETs with strained Si channel, however, strain axes (uniaxial or biaxial) in local areas should be evaluated. This is because the strain induced mobility enhancement significantly depends on not only strain fields and types but also strain axes. In line with this, we focus our efforts on the development of polarized Raman scattering spectroscopy, which utilizes polarization filtering of the scattered light. This paper reports newly developed incident angle dependent polarized Raman spectroscopy, which enables the evaluation of strain axes distributed in Si on insulator (SOI) structures.

2. Experimental Procedure

(001) SOI wafers [top Si: 0.34 μm, buried oxide (BOX): 2 μm] were employed. The top Si was patterned by dry-etching. Subsequently, BOX under the patterned top Si was undercut by wet-etching. Thus, Si bridges (pattern A) or cantilevers (pattern B) (width: 5 μm, length: 20 μm) with supporting bases (100×100 μm^2) were fabricated, as shown in Figs. 1(a) and 1(b), respectively. To induce strain fields in Si, they were covered with SiN (thickness: 0.2 μm) using low-pressure chemical vapor deposition at 700°C. Finally, they were annealed at 1150°C for 30 min in N_2 to enhance the compressive strain [2]. The polarized Raman measurements (laser spot: ~1 $\mu m\phi$, wavelength: 532 nm) were performed for the samples under the backscattering configuration. The measured regions are indicated by the red dots in Figs. 1(a) and 1(b). The measurement setup is schematically shown in Fig. 1(c), where $\mathbf{e_i}$ and θ are the incident light polarization and the angle between $\mathbf{e_i}$ and [100]-axis, respectively.

3. Results and Discussion

Fig. 1(d) shows typical Raman spectra (θ =0^o) obtained from the pattern (A) samples under the parallel ($\mathbf{e_s}$//$\mathbf{e_i}$) and perpendicular ($\mathbf{e_s} \perp \mathbf{e_i}$) polarization configurations, where $\mathbf{e_s}$ is the polarization of the scattered light. In the figure, the spectra obtained without polarization filtering are also shown. These spectra have two peaks at 520.0 and 523.3 cm^{-1}, which are due to the Si-Si vibration mode in the Si substrate and the compressively-strained Si-microstructure, respectively. Since the bridge part is supported by the both-side bases, a uniaxial strain is induced along the x-axis. The strain was evaluated to be 1.3%. These Raman peak intensities depend on the $\mathbf{e_s}$ configuration. It is noticed that the strain peak is clearly detected under $\mathbf{e_s}$//$\mathbf{e_i}$ at θ =0^o, even though this configuration (θ =0^o) is Raman inactive for the strain-free diamond structures [3]. This result suggests that the Raman selection rule known in the strain-free Si should be broken due to the large strain (>1%) induced by the SiN stress-liner.

To investigate these phenomena in more detail, the Raman peak intensities were measured as a function of θ under $\mathbf{e_i}$//$\mathbf{e_s}$ configuration. They are summarized in Fig. 2. It is interesting that the strain induced Raman peak is observed at θ =0^o, even though both of θ =0^o and 90^o are Raman inactive in strain-free Si. This result suggests that the conventionally inactive Raman peak ($\mathbf{e_i}$//$\mathbf{e_s}$ and θ =0, 90^o) appears, when the polarization direction is chosen as parallel to the strain-axis. To examine this speculation, we performed the polarized Raman measurements for pattern (B) samples. The results are shown as a function of θ in Fig. 3, which clearly indicates that strained Raman peaks are observed under both conditions (θ =0^o and 90^o). Since the biaxially-strain is generated at the edge of the cantilever part supported by the one-side base, this result well supports our speculation.

Now, we demonstrate the polarized Raman intensity mapping ($\mathbf{e_i}$//$\mathbf{e_s}$) to show the strain axis distribution. Here, the corner part of the base, indicated by the red square in Fig. 1(a), was used for the demonstration. Figs. 4(a) and 4(b) show the mappings of the strain peak intensity obtained under θ =0^o and 90^o, respectively. It is clear that uniaxially-strains induced along the each edge are highlighted in either Fig. 4(a) or Fig. 4(b). In addition, biaxially-strains at the corner edge are highlighted in both figures. In this way, the strain axis evaluation in local areas becomes possible by using θ dependent polarized Raman spectroscopy.

4. Summary

We have developed θ dependent polarized Raman spectroscopy, which enables strain axis evaluation in strained Si. This is a powerful tool to optimize the strained SOI micro-structures for the advanced LSIs with strained Si channel.

Acknowledgements

We thank Dr. T. Kitamura (Toshiba Semiconductor) for providing the samples. This work was partially supported by a Regional Innovation Cluster Program (Global Type, 2nd Stage) and a Grant-in-Aid for Scientific Research of MEXT, Japan.

References

[1] W. Haensch *et al.*, IBM J. Res. & Dev. **50** (2006) 339.
[2] M. Tanaka *et al.*, Appl. Surf. Sci. **254** (2008) 6226.
[3] K. Mizoguchi and S. Nakashima, J. Appl. Phys. **65** (1989) 2583.

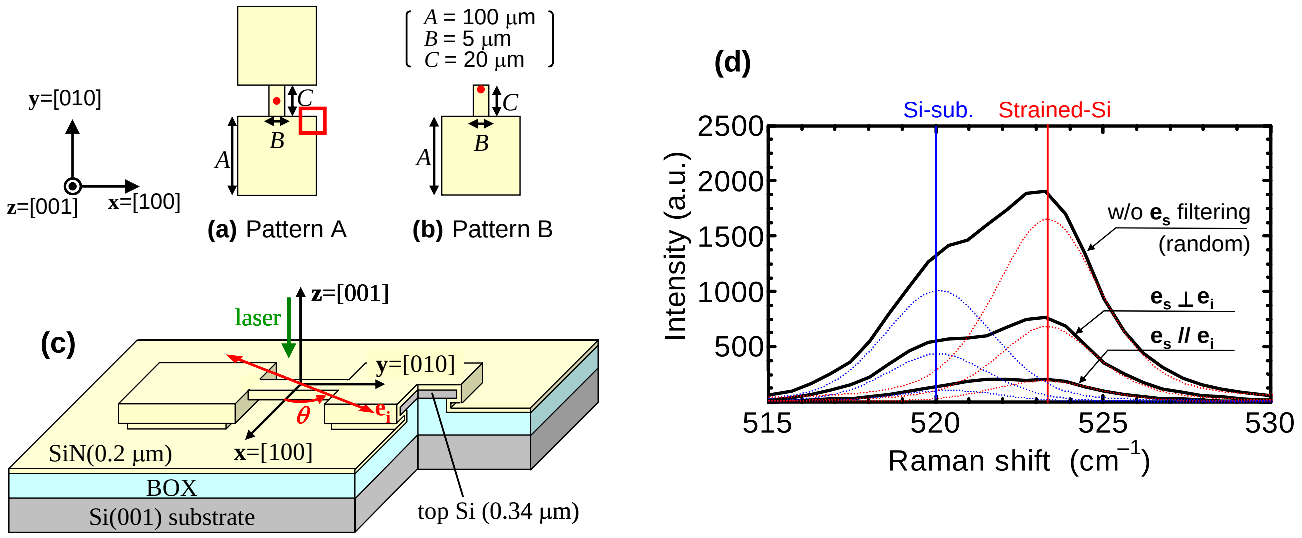

Fig. 1. Plane views of the patterns A (bridge type) (a) and B (cantilever type) (b), measurement setup of polarized Raman scattering spectroscopy (c), and typical Raman spectra obtained for pattern A at $\theta = 0^{\circ}$ (d). The red dots in (a) and (b) indicate the measured positions. The $\mathbf{e}_i$ and $\mathbf{e}_s$ in these figures are the incident and scattered light polarizations, respectively.

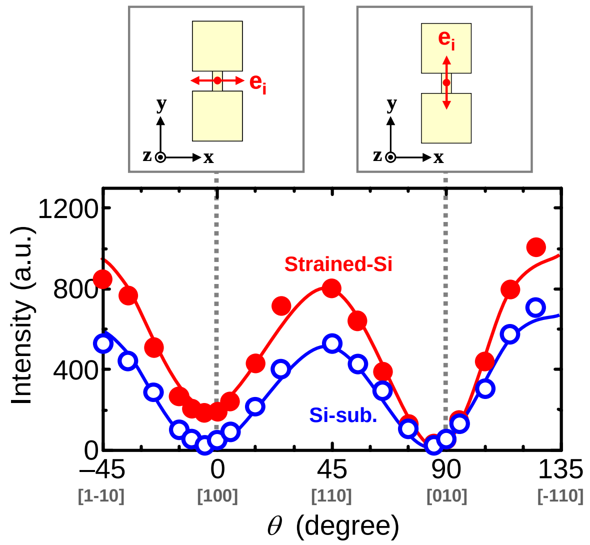

Fig. 2. θ-dependence of polarized Raman peak intensity obtained for pattern A under $\mathbf{e}_i // \mathbf{e}_s$.

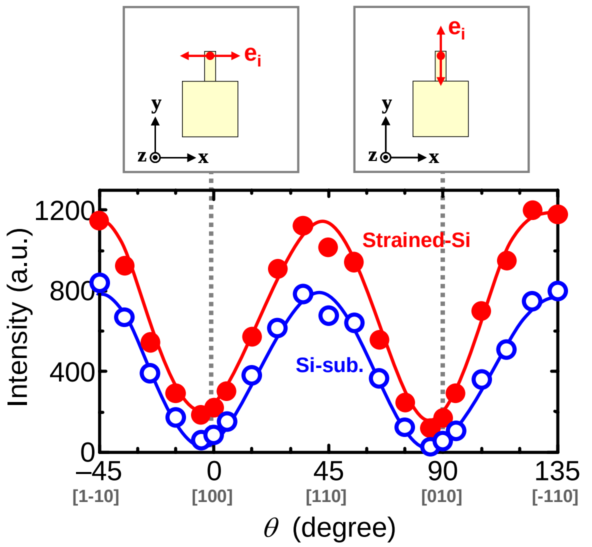

Fig. 3. θ-dependence of polarized Raman peak intensity obtained for pattern B under $\mathbf{e}_i // \mathbf{e}_s$.

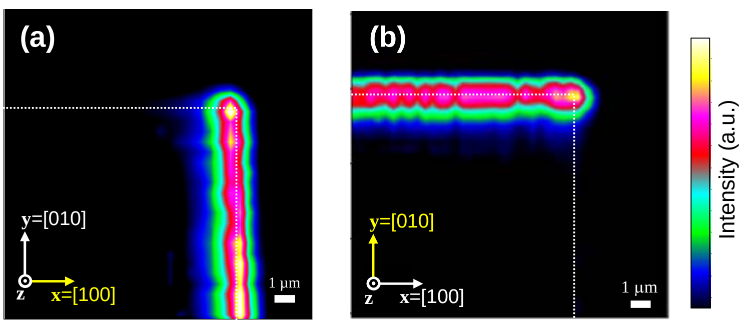

Fig. 4. Mapping of polarized Raman intensity obtained from corner of base under $\mathbf{e}_i // \mathbf{e}_s = [100]$ ($\theta = 0^{\circ}$) (a) and $\mathbf{e}_i // \mathbf{e}_s = [010]$ ($\theta = 90^{\circ}$) (b). The analyzed area is shown by the red box in Fig. 1(a).